IEEE Photonics Journal
An IEEE Photonics Society Publication

Open Access

Watt-Level Continuous-Wave Mode-Locked $Nd:YVO_4$ Laser With $ReSe_2$ Saturable Absorber

Volume 12, Number 5, October 2020

Yuchen Xue
Li Li
Bin Zhang
Ruoxing Wang
Jinhui Cui
Fengjun Tian
Jianzhong Zhang

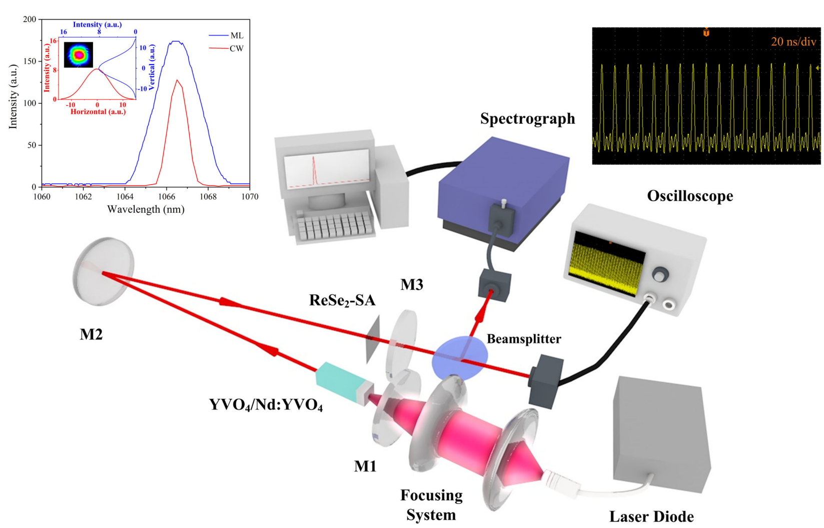

DOI: 10.1109/JPHOT.2020.3022800

IEEE photonics SOCIETY
IEEE

Watt-Level Continuous-Wave Mode-Locked Nd:YVO_4 Laser With $ReSe_2$ Saturable Absorber

Yuchen Xue, Li Li, Bin Zhang, Ruoxing Wang, Jinhui Cui, Fengjun Tian, and Jianzhong Zhang

Key Laboratory of In-Fiber Integrated Optics of Ministry of Education, and College of Physics and Optoelectronic Engineering, Harbin Engineering University, Harbin 150001, China

DOI:10.1109/JPHOT.2020.3022800

Manuscript received July 22, 2020; revised August 28, 2020; accepted September 4, 2020. Date of publication September 8, 2020; date of current version September 18, 2020. This work was supported in part by the National Natural Science Foundation of China (61875043), Fundamental Research Funds for the Central Universities to Harbin Engineering University (HEUCF181115), 111 project to Harbin Engineering University (B13015). Corresponding author: Li Li (email: lylee_heu@hrbeu.edu.cn).

Abstract: We report a $ReSe_2$ passively mode-locked composite YVO_4/Nd:YVO_4 laser at 1.06 μm, which can stably generate pure continuous-wave mode-locking (CWML) operation at watt-level output. $ReSe_2$, as a new type of 2-D transition metal dichalcogenides (TMDs), has the features of weak-layered dependence, broadband saturable absorption, low modulation depth and saturation intensity, which is beneficial to initiate robust CWML mechanism via nonlinear saturable absorption. By employing few-layered $ReSe_2$ as saturable absorber, the nanosecond mode-locked pulses at fundamental repetition rate of 90.37 MHz was obtained experimentally in a composite YVO_4/Nd:YVO_4 laser. The maximum output power in pure CWML operation was as high as 1.1 W. The high-power CWML laser source shows potential applications in time-resolved spectroscopy, telecommunication and detection.

Index Terms: $ReSe_2$, Nd:YVO_4 laser, saturable absorber, continuous-wave mode-locking.

1. Introduction

All-solid-state passively mode-locked lasers with high repetition rate of short pulse output have attracted increasing attention for their advantages in superior stability, high power and quality beam [1]–[3]. They have been widely used in many technical fields such as industrial manufacture, clinical medicine, military and applied science. In order to make the solid-state mode-locked lasers more compact, low cost and easy to operate, nonlinear saturable absorbers were popularly employed as available intra-cavity modulation elements. Traditionally, the passively mode-locking operations were achieved in earlier studies by use of Cr^{4+}:YAG bulk crystals as saturable absorbers [4], [5]. The nonlinear saturable absorption of Cr^{4+}:YAG can be effective only working around 900–1200 nm. Alternatively, semiconductor saturable-absorber mirrors (SESAMs) were exploited to generate passively mode-locked ultrashort pulses [6]–[9]. The complicated preparation of SESAMs involves expensive metal organic chemical vapor deposition (MOCVD) technique with extra high cost. In contrast, the emerging graphene and two-dimensional (2D) noncarbon materials have been explored to be as excellent saturable absorbers, due to their unique nonlinear optical properties involving fast response and broadband operation [10], [11]. Since the first report of graphene passively mode-locked laser in 2009 [10], a variety of graphene-like saturable absorbers have been exploited in passively mode-locking operation [11]. Various novel 2D materials inspired on graphene, such as black phosphorus (BP) [12], [13], topological isolators (TIs) [14], [15], topological Dirac semimetal (TDS) [16], MXene [17], [18], Transition metal monochalcogenides (TMMCs) [19] and transition metal dichalcogenides (TMDs) have been demonstrated to be very promising saturable absorbers for ultrafast lasers as well [20]–[28]. These nanostructured nonlinear optical materials have witnessed a quite rapid development of stable and compact ultrafast sources.

Among the 2D materials, TMDs are a class of compounds denoted by the general form MX_2, where M represents a transition metal (for instance W, Mo, Re, or Ti) and X indicates a chalcogen (for instance S, Se, or Te) [29]. The structure consists of a single plane of transition metal atoms sandwiched between two planes of chalcogen atoms. In fact, there are dozens of potential TMDs owing to permutation and combination between oxygen group elements and transition metal elements. Previously, the group VI TMDs including WS_2, WSe_2, MoS_2 and $MoSe_2$ were particularly studied in experiment for optoelectronics, which enabled TMD passively mode-locking pulse generation in fiber and waveguide laser systems [30]–[34]. In 2014, the pioneering investigation has revealed that MoS_2 of TMDs have saturable absorption properties and can be used as a broadband saturable absorber for ultrafast laser device [20]. Zhang *et al.* fabricated a new type of fibre-pigtailed MoS_2 saturable absorber for passively mode-locked Yb-doped fiber laser and achieved the generation of a pulse duration of 800 ps at 1054 nm [21]. In 2015, Luo *et al.* performed a mode-locked Er-doped fiber laser based on the few-layer $MoSe_2$ film as saturable absorber at 1558 nm [32]. They obtained the repetition-rate of 8.028 MHz and pulse duration of 1.45 ps with the maximum average output power of 0.44 mW. In 2017, Yan *et al.* investigated an erbium-doped fiber laser by using few-layered WS_2 as saturable absorber, which obtained stable passively mode-locking operation [33]. The output pulses had pulse duration of 1.49 ps and repetition rate of 0.487 MHz under the average output power of 62.5 mW. Most recently, Li *et al.* achieved a monolithic Nd:YVO_4 waveguide laser passively mode-locked by WSe_2 at 1064 nm [34]. At the pulse width of 47 ps, the fundamental repetition rate of 6.526 GHz was obtained, when the output power reached the value of 306 mW. The studies of these TMD saturable absorbers mainly focus on fiber lasers or waveguide lasers. Generally, it is difficult to scale up to watt-level high power output of model-locking pulse due to insertion loss and optical damage, especially in continuous wave mode-locking mechanism.

In comparison, TMD passively mode-locked solid-state lasers are likewise facing such challenge, with the limited mode-locking output of at most hundreds of milliwatts. In 2018, Zhang *et al.* reported a passive Q-switched mode-locked (QML) Nd:YVO_4 laser by use of reflective few-layered MoS_2 saturable absorber mirror [35]. A maximum average output power of 198 mW can be obtained with the mode-locked pulse width of 72 ns and repetition rate of 11 MHz. Soon later, Zeng *et al.* made efforts to perform QML operation with MoS_2 saturable absorber in the Nd:YAG laser and improved the output power to watt-level with a repetition rate of 94.72 MHz [36]. Note that the continuous-wave mode-locking (CWML) operation without QML effect was not achieved in those MoS_2 mode-locked solid-state lasers [35], [37]. Particularly, watt-level continuous-wave mode-locking operation with TMD saturable absorbers has not been reported previously.

Recently, rhenium diselenide ($ReSe_2$), as an emerging group VII TMD, was explored to serve as potential nonlinear material due to its distinctive features of the distorted octahedral (1T) lattice structure with triclinic symmetry [30]. The structure-induced anisotropy renders $ReSe_2$ unique performance in anisotropic electronic, optical and mechanical properties, just like that of black phosphorus. This makes $ReSe_2$ different from the layered TMDs (e.g., MoS_2) of conventional 2H lattice structure previously focused on [31]. Few-layered $ReSe_2$ has quite weak interlayer coupling effect which makes the preparation of $ReSe_2$ greatly simplified at low cost. Moreover, $ReSe_2$ shows the advantages of bandgap tunability over graphene, material stability over black phosphorus, and broadband saturation over bulk crystals [10], [11], [30], [31]. Currently, $ReSe_2$ was suggested as saturable absorber for passively Q-switched fiber laser at 1.55 μm, showing comparable Q-switching operation to other TMD-based fiber lasers [38]. By integrating $ReSe_2$ film into monolithic waveguide platform, a waveguide mode-locked laser performed short pulse

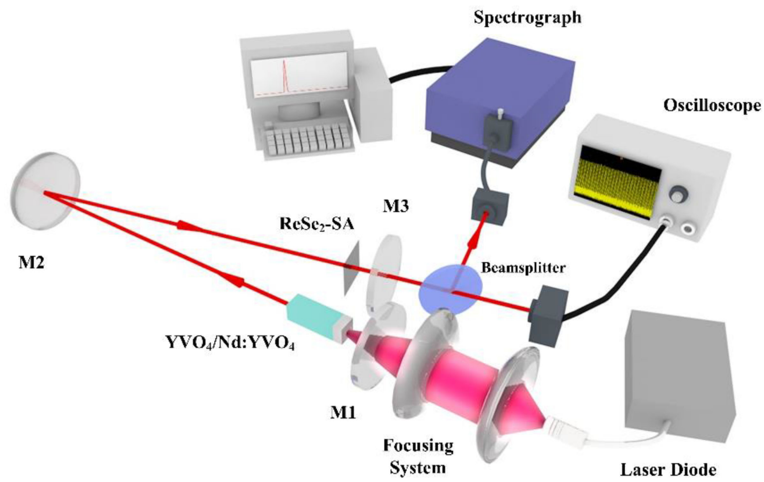

Fig. 1. Experimental setup of $ReSe_2$ passively mode-locked YVO_4/Nd:YVO_4 laser.

output around two hundred milliwatts [39]. In Nd:YAG laser, $ReSe_2$ passively Q-switching operation near room temperature was reported to produce near-repetition rate limit of microsecond pulses at full depth modulation [40]. Additionally at 2–3 μm regions, Q-switched Er:YAP, Tm:YAP and Tm:YLF crystal lasers were achieved in the $ReSe_2$ Q-switching regime [41]–[43]. In 2019, Lee et al presented the investigation of nonlinear optical properties of rhenium diselenide and its application as a femtosecond mode-locker. They obtained the stable soliton pulse with the 862 fs duration in an erbium-doped fiber laser by using a $ReSe_2$ SA. These pioneering works verified that $ReSe_2$ is a novel kind of promising optical material for generating ultrafast lasers in broadband wavelength applications [44]. However, it is worth noting that the emerging $ReSe_2$ has not been exploited as saturable absorber to perform passively mode-locking operation in solid-state bulk lasers yet.

In the paper, we first report a $ReSe_2$ passively mode-locked composite YVO_4/Nd:YVO_4 laser at 1.06 μm, which can stably generate pure continuous-wave mode-locking (CWML) operation at watt-level output. The emerging 2D $ReSe_2$ nanomaterial is confirmed to be beneficial to initiate robust CWML mechanism via nonlinear saturable absorption. By employing few-layered $ReSe_2$ as saturable absorber, the nanosecond mode-locked pulses at the fundamental repetition rate of 90.37 MHz was obtained experimentally in the composite YVO_4/Nd:YVO_4 laser. The maximum output power in pure CWML operation was as high as 1.1 W, successfully scaling up to watt-level CWML in TMD mode-locked lasers.

2. Experimental Setup

$ReSe_2$ passively mode-locked composite YVO_4/Nd:YVO_4 bulk laser was experimentally built. The schematic of experimental setup is shown in Fig. 1. The laser diode end-pumping scheme was adopted for efficient pumping and good mode matching. A 50 W fiber-coupled continuous-wave laser diode at 808 nm was used as the pump source. The fiber core diameter is 400 μm with the numerical aperture of 0.22. A pair of coupled plano-convex lenses can reimage the pump beam into the laser crystal, with 70 mm focusing length. The coupling efficiency of lens group is over 90%. The a-cut YVO_4/Nd:YVO_4 composite crystal (Nd^{3+} $\sim$ 0.3 at %) was employed as the gain medium, with minimizing the possible thermal lensing effects [45], [46]. The cross section of laser crystal is 3 mm $\times$ 3 mm. The lengths of composite YVO_4+Nd:YVO_4 are 2+16 mm. Both end-faces of the crystal were anti-reflection coated with high transmission of T $>$ 99.5% at 1.06 μm and 808 nm. The composite YVO_4/Nd:YVO_4 crystal was wrapped with indium foil and mounted in a water-cooled copper holder for heat dissipation. The temperature was maintained at 290 K by a water cooling equipment. By use of ABCD round-trip matrix method, a stable laser resonator was well designed

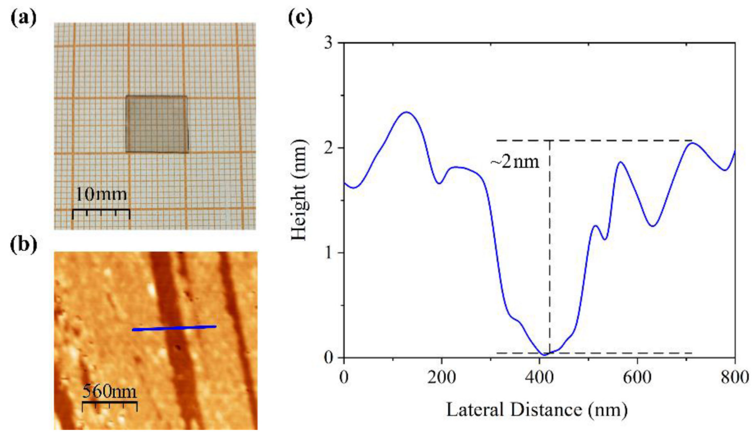

Fig. 2. Characterizations of few-layer $ReSe_2$ sample. (a) Image of $ReSe_2$ element. (b) AFM image of $ReSe_2$ film on sapphire substrate. (c) The height profile diagram of few-layer $ReSe_2$.

as shown in Fig. 1. The V-type folded resonator was constructed with 1.68 m cavity length under the stable condition. The input plane mirror M1 was anti-reflection coated at 808 nm pump and high-reflection coated at 1.06 μm lasing wavelength. The folded mirror M2 is a plano-concave mirror with a 1.0 m radius of curvature, which was high-reflection coated at 1.06 μm band. The output coupling plane mirror, M3, was partial-reflection coated with the transmittance of 4% at 1.06 μm. The distance of M1 to M2 is 850 mm, and that of M2 to M3 is 830 mm, respectively. The V-folding angle is about 12 degrees. The cavity mode radii were calculated to be about 310 μm inside laser crystal and 345 μm on $ReSe_2$ film, respectively. The YVO_4/Nd:YVO_4 crystal was positioned close to input mirror M1, and $ReSe_2$ saturable absorber was located near output mirror M3. The pump beam from the fiber-coupled diode was directly coupled into a lens group to focus into the Nd:YVO_4 crystal with a radius of 800 μm. The pump-to-mode ratio was optimized to be about 1.3 at which the mode-locked laser output can be efficiently scaled up [47]. The beam quality factor of the focused pump was measured to be about $M^2 \approx 6$, and the focusing length was about 70 mm away from the lens end.

The mode-locked output power was measured by a Coherent FieldMaxII laser power meter and an InGaAs photodiode. The mode-locked pulses were recorded by 500 MHz-bandwidth digital oscilloscope and fast InGaAs photodetector with 500 MHz bandwidth. The high-speed InGaAs optical detector can response faster than 300 ps risetime at 800–1750 nm spectra. The spectra were measured by Zolix monochromator with 0.1 nm resolution. The laser beam profile was characterized with a commercial CCD beam analyzer.

3. Experimental Results

The $ReSe_2$ sample used in mode-locking operation was prepared by the chemical vapor deposition (CVD) technology and customized from Sixcarbon Technology (Shenzhen,China). The $ReSe_2$ element is displayed in Fig. 2(a). The few-layer $ReSe_2$ film was evenly deposited on a 10×10 mm^2 double-side optically polished sapphire substrate. The photograph of square wafer in Fig. 2(a) shows its good transparency in sight, with linear transmittance of 83% at 1.06 μm as measured [48]. An atomic force microscopy (AFM) was applied to characterize the transferred layers of the sample. The nanoscale surface topography of $ReSe_2$ was mapped in Fig. 2(b) showing its good quality. Fig. 2(c) shows the height analysis of the transferred layers. The thickness of $ReSe_2$ film was evaluated to be about 2 nm, corresponding to 3–4 layers thick. As one knows, single-layer $ReSe_2$ is 0.6 nm thick, but few-layer $ReSe_2$ can improve optical damage threshold during the mode-locking operation in laser cavity.

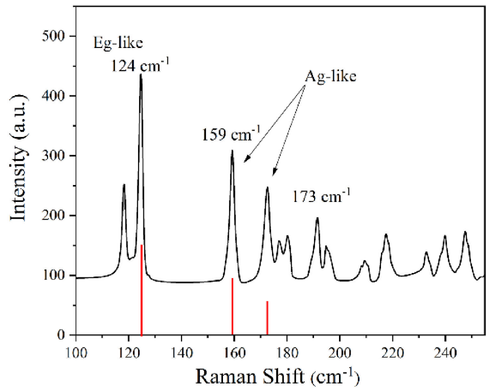

Fig. 3. Measurement of the Raman spectrum for the $ReSe_2$ sample.

Figure 3 shows the measurement of the $ReSe_2$ Raman spectra. Evidently, the Raman scattering measurement indicates three characteristic vibration modes, Eg (124 cm^{-1}) and Ag (159 cm^{-1} and 173 cm^{-1}), which represents in-plane and out-of-plane modes respectively. Other weak peaks emerging in measurement were caused from low symmetry of $ReSe_2$ [48]. In contrast to weak background spectra, the distinct peaks of main Raman shifts at 124 cm^{-1}, 159 cm^{-1} and 173 cm^{-1} imply the uniform few-layer structure of $ReSe_2$ sample [38]. The absorption properties of $ReSe_2$ sample were determined based on the nonlinear absorption model as described in [39], exhibiting stable linear absorption at 1064 nm with insertion loss of about 0.81 dB. The saturation intensity and modulation depth were evaluated to be about 40 μJ/cm^2 and 2.5% respectively, which are suitable to support passively mode-locking mechanism [38], [48]. The two values were calculated from the experiment using the saturable absorption model, which are in accordance with the previous evaluation of the similar samples [38], [48]. In the mode-locked laser, a low modulation depth benefits continuous wave mode-locking operation without passively Q-switched effect. The few-layer $ReSe_2$ results in faster carrier dynamics than SESAM [44]. It is worth noting that in our experiments, no optical damage or degradation of laser performance occurred even when the output pulse energy was at the highest. This means that the intracavity laser intensity on the sample is much less than its damage threshold. For using as saturated absorber, the specific damage threshold of $ReSe_2$ needs further careful measurements. In comparison with other TMDs [37], nonlinear saturation absorption of the $ReSe_2$ performs the favorable condition especially for CWML operation at 1.06 μm.

With the experimental setup of Fig. 1, we measured the average output power of $ReSe_2$ mode-locked Nd:YVO_4 laser versus the absorbed pump power. The experimental data are plotted in Fig. 4(a) with linear fitting lines. The results of Fig. 4(a) indicate that the composite Nd:YVO_4 laser can produce continuous-wave oscillation when the pump power increases around 5 W. The threshold of laser oscillation is higher than the threshold of 2.8 W in CW operation without SA. Suppression of optical conversion efficiency exhibits due to the insertion loss of $ReSe_2$ saturable absorber because Fresnel's reflection from a single surface of sample could be $\sim$7.4%. Upon the pump reaches the critical threshold of 6.7 W, passively mode-locking mechanism starts to initiate due to the nonlinear saturable absorption of $ReSe_2$. When the pumping power is less than 6.7 W in Fig. 4(a), the temporal output characteristics displays typical continuous wave. As the pump power approaches closely to the threshold of 6.7 W, the temporal profile starts the transition from pure continuous wave to mode-locked pulses. Note that the temporal profile and pulse amplitude are unstable around the pump threshold. Further to increase the pump power beyond 6.7 W, the stable CWML operation can be performed as shown in Fig. 5. Robust continuous-wave mode-locking operation carried out in experiment without passively Q-switched effect. The CWML output power can increase near linearly with the pump power. The maximum output of as high as 1.1 W can be

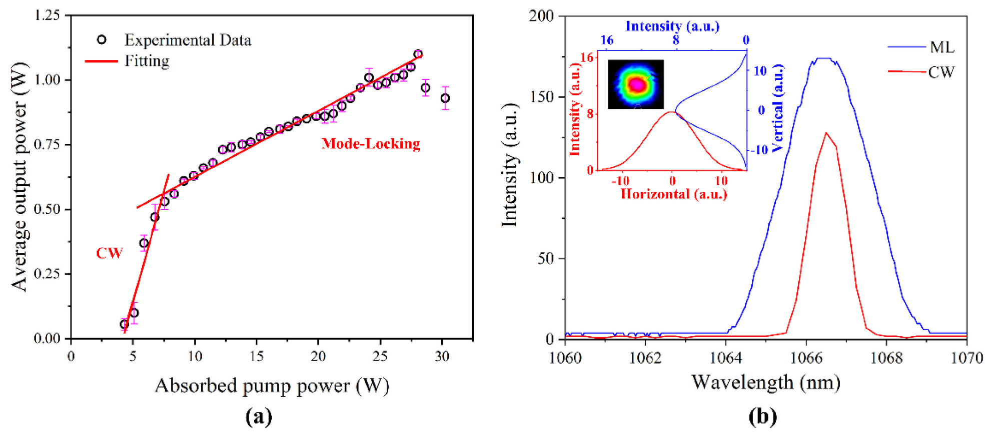

Fig. 4. (a) Average output power of CWML Nd:YVO_4 laser versus the absorbed pump power. By the linear fitting, the slope efficiencies of CW and mode-locking are 16% and 2.5%, respectively. (b) The emission spectrum of the $ReSe_2$ passively mode-locked Nd:YVO_4 laser. Inset: The measured modal profile of CWML output beam.

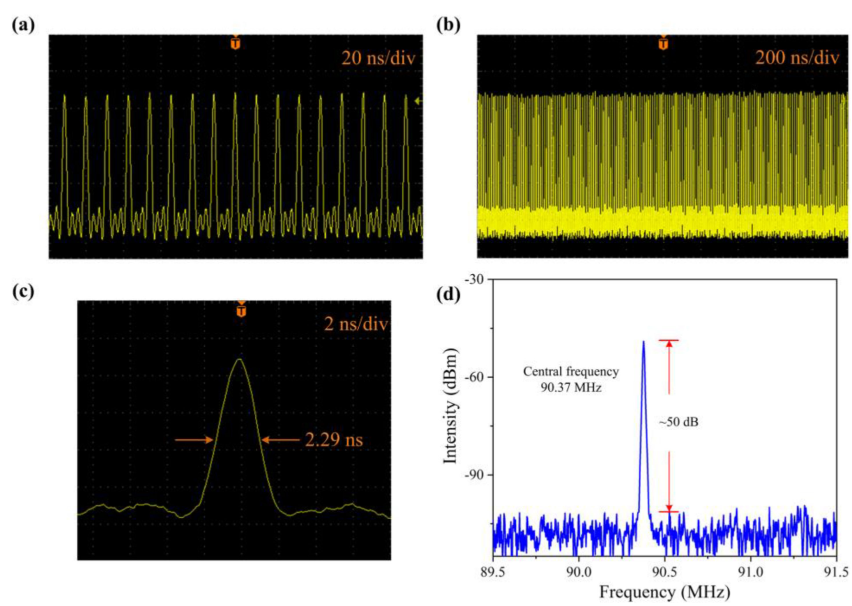

Fig. 5. The continuous-wave mode-locked pulse trains recorded at two different time scale of (a) 20 ns/div and (b) 20 ns/div. (c) The single pulse profile recorded at the time scale of 2 ns/div. (d) The radio frequency spectra showing the signal-to-noise ratio of ~50 dB at 90.37 MHz.

achievable under 28 W pumping, which successfully scales up the $ReSe_2$ CWML laser to watt-level high power output. Note that to the best of our knowledge, this is the first report of watt-level CWML output in graphene/TMDs-based mode-locked fiber/waveguide/bulk lasers reported [5], [10], [22]–[24], [32]–[34].

4. Discussions

As one knows, it is difficult to scale the watt-level output of 2D material-based passively model-locked lasers, especially in continuous wave mode-locking mechanism [35]–[37]. This limitation arises mainly from the insertion loss and optical damage of 2D materials as saturable absorber, as well as thermal effects of laser gain media [49]. Such obstacles have been overcome deliberately in our experiments. Particularly, the diffusion-bonded YVO_4/Nd:YVO_4 crystal was employed to suppress thermal lens effect as discussed in [46], with matching the well-designed V-folded resonator. The $ReSe_2$ element was prepared in good quality with low insertion loss of 0.81 dB and high damage threshold beyond 30 MW/cm^2, while its uniform few-layer structure ensures the moderate saturation intensity and modulation depth to support pure CWML operation. Note that the long crystal of composite YVO_4/Nd:YVO_4 can bring about pulse broadening by virtue of the reduction of spatial-hole-burning effect in the undoped YVO_4 section [49], which is helpful to nanosecond-order mode-locking regime during oscillation and amplification. But the degeneration of CWML performance in power and stability occurs inevitably at high-intensity pumping beyond 30 W. No optical damage was observed in the experiments.

Fig. 4(b) shows the emission spectra of $ReSe_2$ YVO_4/Nd:YVO_4 laser in continuous-wave and mode-locking, respectively. It can be seen the spectral bandwidth of the CWML was broader than the CW operation due to the short pulse output of mode-locking. In experiment, the lasing wavelength was monitored in the region covering the possible Nd^{3+} transitions of $^4F_{3/2}\rightarrow{}^4I_{11/2}$ and $^4F_{3/2}\rightarrow{}^4I_{13/2}$. Only the central wavelength at 1066.5 nm ($^4F_{3/2}\rightarrow{}^4I_{11/2}$) was observed distinctly at single-longitudinal-mode, as shown in Fig. 4(b). The other transition was not observed to produce any lasing emission owing to the specialized resonator with high transmission loss around 1.32 μm of $^4F_{3/2}\rightarrow{}^4I_{13/2}$ [50]. Because $^4F_{3/2}\rightarrow{}^4I_{13/2}$ has a higher fluorescence branching ratio and is the most effective one to generate laser wavelengths in the 1.06 μm band. A further spectroscopic study [51] of Nd:YVO_4 has revealed that there are various emission bands within the $^4F_{3/2}\rightarrow{}^4I_{13/2}$ transition resulting from Stark splitting, corresponding to R1→Y2 (1064 nm) and R2→Y2 (1066.5 nm) Stark sub-level transitions [52]. In addition, the bandwidth of the coated mirror covers 1064 nm and 1066.5 nm. The peaks of the emission cross section spectra are about 1.44×10^{-18} cm^2 at 1064 nm for π-polarization and 2.95×10^{-19} cm^2 at 1066.5 nm for σ-polarization [53]. In our experiment, the laser operated at the wavelength of 1066.5 nm for σ-polarization when the Nd:YVO_4 crystal used in our laser was cut by *a*-axis. The $ReSe_2$ mode-locked Nd:YVO_4 laser at 1066.5 nm basically operates as a typical four-level laser system which is favorable to achieve watt-level high power output without inducing reabsorption losses [45]. At 1.1 W of output power, the laser beam quality was measured as shown in the inset of Fig. 4(b). The transverse mode profile of $ReSe_2$ mode-locked output exhibits in good quality of fundamental electromagnetic mode (TEM_{00}), with symmetric distribution along the horizontal and vertical directions. To assess the beam quality of the CWML Nd:YVO_4 laser, the M^2 factor was measured to be about 4.7 and 4.4 in x and y directions, respectively.

The temporal characteristics of $ReSe_2$ CWML operation were monitored experimentally at a time resolution of 620 ps. The nanosecond short pulses can be definitely observed during the $ReSe_2$ passively mode-locking regime. Fig. 5 displays the observations of CWML pulses at maximum output power of 1.1 W. As shown in Figs. 5(a) and 5(b), typical pulse trains were recorded at the time scale of 20 ns/div and 200 ns/div to reveal the mode-locked state and stability. Clearly, the continuous-wave mode-locked pulses can be generated at full depth of modulation in $ReSe_2$ mode-locked laser, without passively Q-switched effect which previously occurred in other TMDs mode-locked lasers [34]–[36]. The amplitudes of the pulse trains can maintain robust and stable in $ReSe_2$ mode-locking regime, with uniform pulse intervals of about 11 ns. The amplitude fluctuation rate was evaluated less than 2.2% in the experiments. The pure CWML state is closely associated with moderate saturation intensity and ultrafast recovery time of few-layered $ReSe_2$. Single pulse profile was recorded at sufficient sampling rate in measurement, as shown in Fig. 5(c), showing good symmetry of rising and falling traces. The pulse duration can be evaluated to be 2.29 ns of FWHM (full width at half maximum), which is comparable to those of previous TMDs passively mode-locked lasers [34], [35], [54]–[56]. The standard deviation of pulsewidth is 0.05. Note that the pulse duration of 2.29 ns is wider than common CWML ultrashort pulses. CWML pulse widths are usually limited to wider scales because of a narrow gain linewidth of Nd^{3+} doped crystal [6]. In addition, although the diffusion-bonded crystal, YVO_4/Nd:YVO_4, can usefully reduce the thermal effects, the mode-locked pulse width is usually broader than that obtained with the conventional

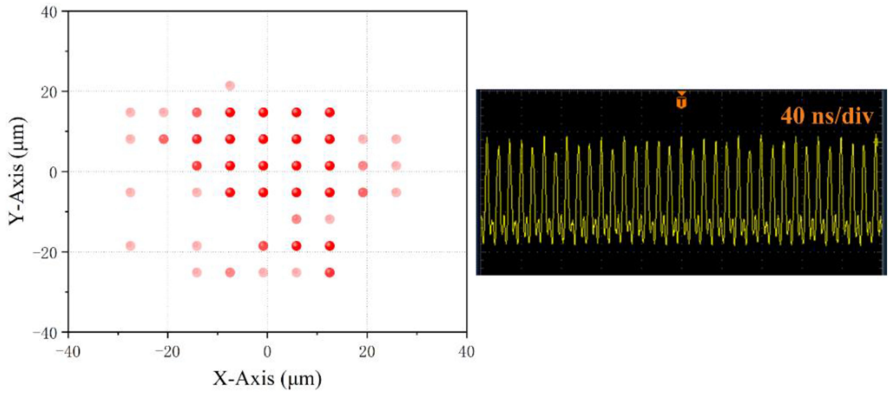

Fig. 6 (a) The changes of output beam position in transverse space monitored for half an hour under random external perturbations. (b) Instability of CWML pulse trains recorded in experiments during random disturbances.

crystal [49]. The nanosecond mode-locking operation depends on the employment of long composite YVO_4/Nd:YVO_4 and the reduced spatial-hole-burning effect [49]. It needs to mention that the obtained mode-locked pulses were measured by a 500 MHz bandwidth of oscilloscope which is adequate to get nanoseconds pulse width [35], [54]. When further to reveal the instantaneous details of continuous-wave mode-locked pulses, it is required to employ autocorrelator instead of oscilloscope [6], [33]. As shown in Fig. 5(d), the radio frequency spectra analysis was carried out in $ReSe_2$ CWML operation. The fundamental frequency was confirmed to be at 90.37 MHz with high signal-to-noise ratio up to 50 dB, indicating good stability of CWML pulse repetition rate. The standard deviation of fundamental frequency is 0.57 based on experimental data analysis. Note that under high pump powers, the single pulse output might be converted into a bunched pulse state due to Kerr nonlinearity [57]. So the temporal shape of the output pulses was resolved with the combined use of a high speed oscilloscope and a fast photodetector. No bound multiple pulses were generated in the experiment.

Additionally, the stability of $ReSe_2$ mode-locked YVO_4/Nd:YVO_4 laser against external perturbations was discussed by applying random vibrations to the experimental platform. The applied vibrations can cause random perturbations resulting in drift of output beam position in transverse space. The transverse distribution of the drifted beam position can be monitored by position detector to intuitively reflect the strength of perturbations. As shown in Fig. 6(a), the changes of output beam position were monitored for half an hour under random external perturbations, with maximum disturbance strength around ± 20 μm. In the scatter diagram of Fig. 6(a), the color depth indicates the occurrence frequency of output beam position at the position (x y). During the whole disturbance, the $ReSe_2$ mode-locked YVO_4/Nd:YVO_4 laser can maintain pure CWML state without breaking off the mode-locking mechanism, as shown in Fig. 6(b). Once the external perturbations result in a large lateral drift-magnitude over ± 30 μm, the CWML pulses can perform instability in time and amplitude inevitably. In the external perturbation stability test of Fig. 6, the pumping power is 28 W, with the laser output power of 1.1 W. During the test period, the laser output intensity performed slight reduction relative to the original output intensity, but without serious degradation. The perturbation test suggests that the $ReSe_2$ mode-locked YVO_4/Nd:YVO_4 laser has good anti-disturbance performance in watt-level CWML operation. In experiment, the CW operation of 1.1 W output power can last over 30 minutes. Several repeated tests were conducted to perform the watt-level power stability. Such stability is associated with the employment of the bonding laser crystal and temperature controlling system which can ensure the suppression of heat accumulation and thermal lens effect.

5. Conclusion

In conclusion, $ReSe_2$ passively mode-locked composite YVO_4/Nd:YVO_4 laser at 1.06 μm has been demonstrated experimentally. Pure continuous-wave mode-locking operation at watt-level output has been performed firstly by exploiting a new kind of 2D material $ReSe_2$ to initiate robust CWML regime via nonlinear saturable absorption. The maximum output power in pure CWML operation has been obtained as high as 1.1 W, successfully scaling up to watt-level CWML state over the previous TMD mode-locked lasers. The fundamental frequency is at 90.37 MHz with high signal-to-noise ratio of 50 dB, showing good stability in time and amplitude. The high-power CWML laser source shows potential applications in time-resolved spectroscopy, telecommunication and detection.

References

[1] R. L. Byer, "Diode laser-pumped solid-state lasers," *Science*, vol. 239, no. 4841, pp. 742–747, 1988.
[2] Y. F. Chen, S. W. Tsai, and S. C. Wang, "High-power diode-pumped Q-switched and mode-locked Nd:YVO4 laser with a Cr4+:YAG saturable absorber," *Opt. Lett.*, vol. 25, no. 19, pp. 1442–1444, 2000.
[3] Y. X. Bai *et al.*, "Passively Q-switched Nd:YVO4 laser with a Cr4+:YAG crystal saturable absorber," *Appl. Opt.*, vol. 36, no. 12, pp. 2468–2472, 1997.
[4] Y. X. Leng, H. H. Lu, L. H. Lin, and Z. Z. Xu, "Active-passive mode-locking using Cr4+:YAG crystal as saturable absorber," *Opt. Laser Technol.*, vol. 33, pp. 403–407, 2001.
[5] J. P. Qiao *et al.*, "Dual-loss modulated Nd:GGG laser with Cr4+:YAG and GaAs," *Opt. Laser Technol.*, vol. 64, pp. 324–327, 2014.
[6] S. D. Liu *et al.*, "High-power femtosecond pulse generation in a passively mode-locked Nd:SrLaAlO4 laser," *Appl. Phys. Express*, vol. 9, no. 7, 2016, Art. no. 072701.
[7] S. D. Liu *et al.*, "Femtosecond pulse generation with an a-cut Nd:CaYAlO4 disordered crystal," *Appl. Opt.*, vol. 55, no. 27, pp. 7659–7662, 2016.
[8] J. J. Liu *et al.*, "Efficient continuous-wave and passive Q-switched mode-locked Er3+:CaF2–SrF2 lasers in the mid-infrared region," *Opt. Lett.*, vol. 43, no. 10, pp. 2418–2421, 2018.
[9] J. J. Liu *et al.*, "1886-nm mode-locked and wavelength tunable Tm-doped CaF2 lasers," *Opt. Lett.*, vol. 44, no. 1, pp. 134–137, 2019.
[10] H. Zhang, D. Y. Tang, L. M. Zhao, Q. L. Bao, and K. P. Loh, "Large energy mode locking of an erbium-doped fiber laser with atomic layer graphene," *Opt. Express*, vol. 17, no. 20, pp. 17630–17635, 2009.
[11] B. Guo, "2D noncarbon materials-based nonlinear optical devices for ultrafast photonics," *Chin. Opt. Lett.*, vol. 16, no. 2, 2018, Art. no. 020004.
[12] K. i. Park, J. Lee, Y. T. Lee, W. K. Choi, J. H. Lee, and Y. W. Song, "Black phosphorus saturable absorber for ultrafast mode-locked pulse laser via evanescent field interaction," *Ann. Phys.*, vol. 527, no. 11–12, pp. 770–776, 2015.
[13] J. Sotor, G. Sobon, M. Kowalczyk, W. Macherzynski, P. Paletko, and K. M. Abramski, "Ultrafast thulium-doped fiber laser mode locked with black phosphorus," *Opt. Lett.*, vol. 40, no. 16, pp. 3885–3888, 2015.
[14] J. Sotor, G. Sobon, W. Macherzynski, P. Paletko, K. Grodecki, and K. M. Abramski, "Mode-locking in Er-doped fiber laser based on mechanically exfoliated Sb2Te3 saturable absorber," *Opt. Mater. Express*, vol. 4, no. 1, pp. 1–6, 2014.
[15] J. Lee, J. Koo, Y. M. Jhon, and J. H. Lee, "A femtosecond pulse erbium fiber laser incorporating a saturable absorber based on a bulk-structured Bi2Te3 topological insulator," *Opt. Express*, vol. 22, no. 5, pp. 6165–6173, 2014.
[16] C. H. Zhu *et al.*, "A robust and tuneable mid-infrared optical switch enabled by bulk Dirac fermions," *Nat. Commun.*, vol. 8, 2017, Art. no. 14111.
[17] Y. I. Jhon *et al.*, "Metallic MXene saturable absorber for femtosecond mode-locked lasers," *Adv. Mater.*, vol. 29. no. 40, 2017, Art. no. 1702496.
[18] X. T. Jiang *et al.*, "Boradband nonlinear photonics in few-layer MXene Ti3C2Tx (T = F, O, or OH)," *Laser Photon. Rev.*, vol. 12, no. 2, 2018, Art. no. 1700229.
[19] Y. I. Jhon, J. Lee, M. Seo, J. H. Lee, and Y. M. Jhon, "van der Waals layered tin selenide as highly nonlinear ultrafast saturable absorber," *Adv. Opt. Mater.*, vol. 7, no. 10, 2019, Art. no.1801745.
[20] S. X. Wang *et al.*, "Broadband few-layer MoS2 saturable absorber," *Adv. Mater.*, vol. 26, no. 21, pp. 3538–3544, 2014.
[21] H. Zhang *et al.*, "Molybdenum disulfide (MoS2) as a broadband saturable absorber for ultra-fast photonics," *Opt. Express*, vol. 22, no. 6, pp. 7249–7260, 2014.
[22] X. L. Sun *et al.*, "Passively mode-locked 1.34 μm bulk laser based on few-layer black phosphorus saturable absorber," *Opt. Express*, vol. 25, no. 17, pp. 20025–20032, 2017.
[23] C. J. Zhao *et al.*, "Ultra-short pulse generation by a topological insulator based saturable absorber," *Appl. Phys. Lett.*, vol. 101, 2012, Art. no. 211106.
[24] B. L. Wang *et al.*, "Topological insulator simultaneously Q-switched dual-wavelength Nd:Lu2O3 laser," *IEEE Photon. J.*, vol. 6, no. 3, Jun. 2014, Art. no. 1501007.
[25] B. Xu *et al.*, "Passively Q-switched Nd:YAlO3 nanosecond laser using MoS_2 as saturable absorber," *Opt. Express*, vol. 22, no. 23, pp. 28934–28940, 2014.
[26] C. Cheng, H. L. Liu, Y. Tan, J. R. V. de Aldana, and F. Chen, "Passively Q-switched waveguide lasers based on two-dimensional transition metal diselenide," *Opt. Express*, vol. 24, no. 10, pp. 10385–10390, 2016.

[27] B. H. Chen, X. Y. Zhang, K. Wu, H. Wang, J. Wang, and J. P. Chen, “Q-switched fiber laser based on transition metal dichalcogenides MoS2, MoSe2, WS2, and WSe2,” *Opt. Express*, vol. 23, no. 20, pp. 26723–26737, 2015.

[28] H. F. Lin, W. Z. Zhu, R. Z. Mu, H. Y. Zhang, and F. B. Xiong, “Q-switched dual-wavelength laser at 1116 and 1123 nm using WS2 saturable absorber,” *IEEE Photon. Technol. Lett.*, vol. 30, no. 3, pp. 285–288, Feb. 2018.

[29] K. F. Mak and J. Shan, “Photonics and optoelectronics of 2D semiconductor transition metal dichalcogenides,” *Nat. Photon.*, vol. 10, no. 4, pp. 216–226, 2016.

[30] M. Hafeez, L. Gan, A. S. Bhatti, and T. Y. Zhai, “Rhenium dichalcogenides (ReX2, X = S or Se): An emerging class of TMDs family,” *Mater. Chem. Front.*, vol. 1, pp. 1917–1932, 2017.

[31] Q. H. Wang, K. Kalantar-Zadeh, A. Kis, J. N. Coleman, and M. S. Strano, “Electronics and optoelectronics of two-dimensional transition metal dichalcogenides,” *Nat. Nanotechnology*, vol. 7, no. 11, pp. 699–712, 2012.

[32] Z. Q. Luo *et al.*, “Nonlinear optical absorption of few-layer molybdenum diselenide (MoSe2) for passively mode-locked soliton fiber laser,” *Photon. Res.*, vol. 3, no. 3, pp. A79–A86, 2015.

[33] P. G. Yan *et al.*, “Large-area tungsten disulfide for ultrafast photonics,” *Nanoscale*, vol. 9, no. 5, pp. 1871–1877, 2017.

[34] Z. Q. Li, R. Li, C. Pang, Y. X. Zhang, H. H. Yu, and F. Chen, “WSe_2 as a saturable absorber for multi-gigahertz Q-switched mode-locked waveguide lasers,” *Chin. Opt. Lett.*, vol. 17, no. 2, 2019, Art. no. 020013.

[35] G. Zhang, Y. G. Wang, Z. D. Chen, Z. Y. Jiao, and Y. J. Zeng, “High repetition rate QML YVO4/Nd:YVO4/YVO4 laser with a reflective MoS2-SA,” *IEEE Photon. Technol. Lett.*, vol. 30, no. 6, pp 553–556, Mar. 2018.

[36] Y. J. Zeng *et al.*, “Watt-level passively Q-switched and mode-locked Nd:YAG laser with a reflective MoS2 saturable absorber,” *Opt. Laser Technol.*, vol. 108, no. 355–359, 2018.

[37] Q. Wen, L. Q. Sun, Y. G. Wang, E. Y. Zhang, and Q. Tian, “An effective method for designing insensitive resonator of continuous-wave passively mode-locked laser,” *Opt. Express*, vol. 17, no. 11, pp. 8956–8961, 2009.

[38] L. Du *et al.*, “Few-layer rhenium diselenide: An ambient-stable nonlinear optical modulator,” *Opt. Mater. Express*, vol. 8, no. 4, pp. 926–935, 2018.

[39] Z. Q. Li, N. N. Dong, Y. X. Zhang, J. Wang, H. H. Yu, and F. Chen, “Mode-locked waveguide lasers modulated by rhenium diselenide as a new saturable absorber,” *APL Photon.*, vol. 3, no. 8, 2018, Art. no. 080802.

[40] Y. C. Xue *et al.*, “$ReSe_2$ passively Q-switched Nd:Y3Al5O12 laser with near repetition rate limit of microsecond pulse output,” *Opt. Commun.*, vol. 445, pp. 165–170, 2019.

[41] Y. P. Yao *et al.*, “Highly efficient continuous-wave and ReSe2 Q-switched $\sim$3 μm dual-wavelength Er:YAP crystal lasers,” *Opt. Lett.*, vol. 44, no. 11, pp. 2839–2842, 2019.

[42] Y. P. Yao *et al.*, “The energy band structure analysis and 2 μm Q-switched laser application of layered rhenium diselenide,” *RSC Adv.*, vol. 9, no. 25, pp. 14417–14421, 2019.

[43] C. Li, Y. X. Leng, and J. J. Huo, “ReSe2 as a saturable absorber in a Tm-doped yttrium lithium fluoride (Tm:YLF) pulse laser,” *Chin. Opt. Lett.*, vol. 17, no. 1, 2019, Art. no. 011402.

[44] J. Lee, K. Lee, S. Kwon, B. Shin and J. H. Lee, “Investigation of nonlinear optical properties of rhenium diselenide and its application as a femtosecond mode-locker,” *Photon. Res.*, vol. 7, no. 9, pp. 984–993 2019.

[45] Y. J. Wang, W. H. Yang, H. J. Zhou, M. R. Huo, and Y. H. Zheng, “Temperature dependence of the fractional thermal load of Nd:YVO4 at 1064 nm lasing and its influence on laser performance,” *Opt. Express*, vol. 21, no. 15, pp. 18068–18078, 2013.

[46] A. Ahmadi, A. Avazpour, H. Nadgaran, and M. Mousavi, “Numerical analysis and experimental study of thermal lensing of standard and composite Nd:YVO4 crystal with temperature dependence of thermal conductivity tensor,” *Laser Phys.*, vol. 28, no. 10, 2018, Art. no. 105002.

[47] Y. F. Chen, “Pump-to-mode size ratio dependence of thermal loading in diode end-pumped solid-state lasers,” *J. Opt. Soc. Am. B.*, vol. 17, no. 11, pp. 1835–1840, 2000.

[48] C. Li, Y. X. Leng, and J. J. Huo, “Diode-pumped solid-state Q-switched laser with rhenium diselenide as saturable absorber,” *Appl. Sci.*, vol. 8, no. 10, 2018, Art. no. 1753.

[49] Y. J. Huang, Y. P. Huang, H. C. Liang, K. W. Su, Y. F. Chen, and K. F. Huang, “Comparative study between conventional and diffusion-bonded Nd-doped vanadate crystals in the passively mode-locked operation,” *Opt. Express*, vol. 18, no. 9, pp. 9518–9524, 2010.

[50] Y. F. Chen, “cw dual-wavelength operation of a diode-end-pumped Nd:YVO4 laser,” *Appl. Phys. B-Lasers O.*, vol. 70, pp. 475–478, 2000.

[51] S. Yoichi and T. Takunori, “Comparative study on the smectroscopic properties of Nd: GdVO4 and Nd: YVO4 with hybrid process,” *IEEE J. Sel. Top. Quant. Electron.*, vol. 11, no. 3, pp. 613–620, May/Jun. 2005.

[52] S. J. Zhou, P. Gu, X. L. Li, and S. B. Liu, “Continuous wave dual-wavelength Nd:YVO4 laser working at 1064 and 1066 nm,” *Chin. Opt. Lett.*, vol. 15, no. 7, 2017, Art. no. 071401.

[53] S. Yoichi and T. Takunori, “Spectroscopic properties of neodymium-doped yttrium orthovanadate single crystals with high-resolution measurement,” *Jpn. J. Appl. Phys.*, vol. 41, no. 10, pp. 5999–6002, 2002.

[54] J. Liu, Y. G. Wang, Z. S. Qu, L. H. Zheng, L. B. Su, and J. Xu, “Graphene oxide absorber for 2 μm passive mode-locking Tm:YAlO3 laser,” *Laser Phys. Lett.*, vol. 9, no. 1, pp. 15–19, 2012.

[55] S. C. Xu *et al.*, “Watt-level passively Q-switched mode-locked YVO4/Nd:YVO4 laser operating at 1.06 μm using graphene as a saturable absorber,” *Opt. Laser Technol.*, vol. 56, pp. 393–397, 2014.

[56] Q. J. Huang, W. Ji, S. Z. Jiang, D. J. Feng, and X. F. Chen, “Graphene absorber for passive mode-locking Nd: YVO4 laser,” *Optik*, vol. 126, no. 19, pp. 1844–1847, 2015.

[57] S. F. Lin, Y. H. Lin, C. H. Cheng, Y. C. Chi, and G. R. Lin, “Stability and chirp of tightly bunched solitons from nonlinear polarization rotation mode-locked erbium-doped fiber lasers,” *J. Lightw. Technol.*, vol. 34, no. 22, pp. 5118–5128, Nov. 2016.